Energetics and Structures of Adamantane and the 1- and 2-Adamantyl Radicals, Cations, and Anions

Ge Yan, Nicole R. Brinkmann, and Henry F. Schaefer III*

Center for Computational Quantum Chemistry, University of Georgia, Athens, Georgia 30602-2525

Received: June 10, 2003; In Final Form: August 19, 2003

Equilibrium structures and harmonic vibrational frequencies were computed for adamantane (Ad), the 1- and 2-adamantyl radicals (1-Ad•, 2-Ad•), cations (1-Ad$^+$, 2-Ad$^+$), and anions (1-Ad$^-$, 2-Ad$^-$). Ionization potentials and electron affinities of Ad, 1-Ad• and 2-Ad• have been predicted using four different density functional and hybrid Hartree−Fock/density functional methods. The equilibrium structure of adamantane (T_d symmetry) is in excellent agreement with electron diffraction experiments. 1-Ad• and 1-Ad$^-$ are predicted to lie about 4 kJ mol^{-1} below their 2-isomers, while 1-Ad$^+$ is predicted to lie 47 kJ mol^{-1} below 2-Ad$^+$. For 1-Ad•, 1-Ad$^+$, and 1-Ad$^-$, C_{3v} structures are found to be the minima, while a C_s structure lies lowest for 2-Ad•, 2-Ad$^+$, and 2-Ad$^-$. The final predicted adiabatic ionization potentials for the radicals are 6.22 (1-Ad•) and 6.70 eV (2-Ad•). The vertical radical ionization potentials are necessarily larger: 6.85 (1-Ad•) and 7.08 eV (2-Ad•). The predicted adiabatic electron affinities are all negative: −0.13 (1-Ad•) and −0.13 eV(2-Ad•). The vertical electron affinities are −0.28 (1-Ad•) and −0.37 eV(2-Ad•). The vertical detachment energies are 0.07 (1-Ad$^-$) and 0.22 eV(2-Ad$^-$).

I. Introduction

Adamantane has been the subject of much chemical interest because of its highly symmetric cage structure. Schleyer's 1957 synthesis[1] transformed adamantane from an exotic species into one of the staples of organic chemistry. Adamantane and its derivatives have a broad range of chemical,[2,3] polymer,[4,5] and pharmaceutical[6−9] applications. Compounds containing adamantyl radicals are useful catalysts for many chemical reactions,[2,3] such as the refining of halogen atoms and preparation of heterogeneous bimetallic catalysts. The rigid, spherical structure of adamantane reduces interchain interaction in polymers and helps the synthesis of polymers,[4,5] such as MAE-PPV. Adamantane-containing molecules have also been found to have antiviral activity. They have been used in the treatment of influenza,[6] HIV-1,[7] leukemia and deafness,[8] and many other diseases.[9]

Adamantane and its derivatives have been the subject of many studies, both experimental and theoretical. The molecular structure of adamantane was determined by Hargittai, et al. in 1972 using gas-phase electron diffraction.[10] Adamantane has also been studied with two-dimensional Penning ionization electron spectroscopy,[11] by which the adiabatic (IP_a) and vertical (IP_v) ionization potentials were reported as 9.40 and 9.67 eV, respectively. Valuable information concerning the 1- and 2-adamantyl radicals (1-Ad• and 2-Ad•) was obtained by Kruppa and Beauchamp using photoelectron spectroscopy,[12] and the IP_a and IP_v were found for each system (IP_a, 6.21 ± 0.03 eV, IP_v, 6.36 ± 0.05 eV for 1-Ad•; IP_a, 6.73 ± 0.03 eV, IP_v, 6.99 ± 0.05 eV for 2-Ad•). ESR studies have been performed on 2-Ad•,[13] and a planar radical site was suggested. Electron impact appearance energies were used to measure the heats of formation of the 1- and 2-adamantyl cations (1- and 2-Ad$^+$) and 2-Ad•,[14] and these were recently computed using the G2(MP2) methodology. [15] The Raman and IR spectra of adamantane and 2-adamantanone were computed using density functional theory.[16] Dutler, Rauk, Sorensen, and Whitworth used the MP2/6-31G* method to study 2-Ad$^+$ and proposed that the ground electronic state has C_s symmetry.[17] However, very little experimental research has been reported for the adamantyl anions, because of their apparent general instability. Complete molecular structures for the adamantyl radicals and anions are not available. Theoretical predictions on the properties of these species can thus provide valuable information concerning their relative stabilities and reactivities.

Density functional theory (DFT) has been shown to be a relatively inexpensive and reliable theoretical method for predicting ionization potentials (IPs) as well as electron affinities (EAs).[18,19] Using a moderate DZP++ basis set, DFT has been exhaustively tested and shown to predict molecular EAs to within 0.15 eV of the experimentally reported values on average. [19] In the present study we predicted the structures, vibrational frequencies, and relative energies of adamantane, 1- and 2-Ad•, 1- and 2-Ad$^+$, and 1- and 2-Ad$^-$ as well as IPs and EAs of 1- and 2- Ad• to investigate the relative stabilities and reactivity of these species.

II. Methods

The DFT quantum chemical computations were performed on Ad, 1- and 2-Ad•, 1- and 2-Ad$^+$, and 1- and 2-Ad$^-$ using the Gaussian 94 program package.[20] Several gradient-corrected functionals, denoted B3LYP, BHLYP, BLYP, and BP86, were used to compute the geometries, energies, and harmonic vibrational frequencies. Energies were converged to at least 10^{-6} hartrees in the self-consisted-field procedures, although the absolute accuracy may be somewhat lower, due to errors inherent in the numerical integration procedures.

The different functionals used may be described as follows. B3LYP is a hybrid Hartree−Fock and density functional theory (HF/DFT) method using Becke's three-parameter gradient-corrected exchange functional (B3)[21] with the Lee−Yang−Parr's correlation functional (LYP).[22] The BHLYP functional combines Becke's half-and-half exchange functional[23] (BH) with

10.1021/jp0307304 CCC: $25.00
Published on Web 10/11/2003

the LYP correlation functional and is a HF/DFT method. BLYP uses Becke's 1988 exchange function (B)[24] and the LYP functional, and BP86 is formed from the Becke's exchange functional (B) and the 1986 correlation correction of Perdew (P86).[25] Geometries were optimized for each molecular species with each functional using analytic gradient techniques. Residual Cartesian gradients were less than 1.5×10^{-5} hartrees/Bohr. Stationary points found in optimizations were confirmed as minimum by computing the harmonic vibrational frequencies using analytic second derivatives with each functional.

A double-ζ basis set with polarization and diffuse functions, denoted DZP++, was utilized in this study. The basis set was constructed from the Huzinage−Dunning[26,27] set of contracted double-ζ Gaussian functions. Added to this was one set of p-type polarization functions for each H atom and one set of d-type polarization functions for each C atom [$\alpha_p(H) = 0.75$ and $\alpha_d(C) = 0.75$]. To complete the DZP++ basis, the above set of functions was augmented with an "even-tempered" s diffuse function for each H atom and "even-tempered" s and p diffuse functions for each C atom with orbital exponents determined by the formula expressed by Lee and Schaefer[28] [$\alpha_s(H) = 0.04415$, $\alpha_s(C) = 0.04302$, and $\alpha_p(H) = 0.03629$]. The final contraction scheme for this basis is H [5s1p/3s1p] and C [10s6p1d/5s3p1d].

IPs and EAs were evaluated as differences in total energies between molecular species. The classical adiabatic IPs are defined as

$$\mathrm{IP_a} = E_{(\text{optimized cation})} - E_{(\text{optimized radical})}$$

the classical adiabatic IPs with zero-point corrections are

$$\mathrm{IP_a} = E_{(\text{zero-point corrected cation})} - E_{(\text{zero-point corrected radical})}$$

and the vertical IPs are determined by

$$\mathrm{IP_v} = E_{(\text{cation at optimized radical geometry})} - E_{(\text{optimized radical})}$$

The classical adiabatic EAs are defined as

$$\mathrm{EA_a} = E_{(\text{optimized radical})} - E_{(\text{optimized anion})}$$

the vertical EAs are

$$\mathrm{EA_v} = E_{(\text{optimized radical})} - E_{(\text{anion at optimized radical geometry})}$$

and the vertical detachment energies were computed via

$$\mathrm{VDE} = E_{(\text{radical at optimized anion geometry})} - E_{(\text{optimized anion})}$$

III. Results and Discussion

A. Structures and Energetics. Optimized structures of Ad, 1- and 2-Ad$^{\bullet}$, Ad$^+$, and Ad$^-$ with all functionals are shown in Figures 1−3, and geometrical parameters are summarized in Tables 1−7. The total and relative ground-state energies of Ad, 1- and 2-Ad$^{\bullet}$, Ad$^+$, and Ad$^-$ are summarized in Tables 8 and 9.

The theoretical geometry of the T_d symmetry adamantane (Table 1) is in excellent agreement with the electron diffraction experiments. The B3LYP predicted geometry is the closest to experimental values, with C−C and C−H bond lengths of 1.544 and 1.100 Å, respectively, and the C−C$_{sec}$−C and C−C$_{ter}$−C bond angles of 109.7 and 109.4°, respectively.

For the molecular anion 1-Ad$^-$ (Table 4), the ground state is found to possess C_{3v} symmetry. The geometry change at the formal anionic center is rather small compared to neutral adamantane. At the DZP++ B3LYP level, The C$^-$−C$_\alpha$ bond length was shortened by 0.019 Å and the C$_\alpha$−C$^-$−C$_\alpha$ angle is decreased by 0.5° upon the removal of the proton from Ad. The C$_\alpha$−C$_\beta$ bond length is increased by 0.014 Å and the C$^-$−C$_\alpha$−C$_\beta$ angle is decreased by 1.5°.

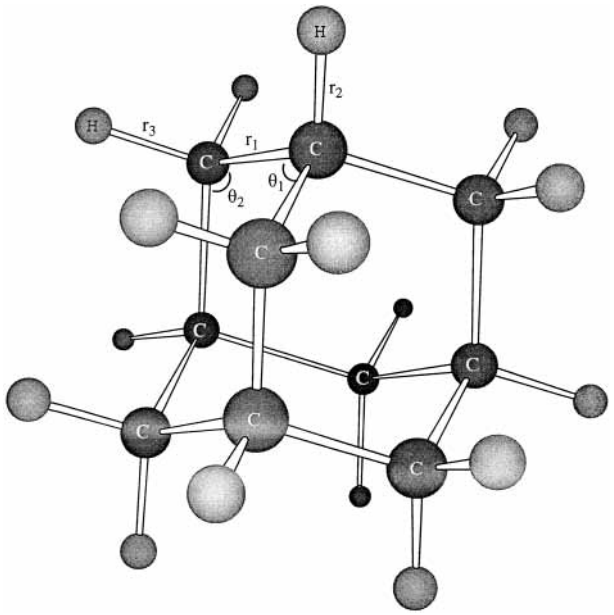

Figure 1. Adamantane ($C_{10}H_{16}$), T_d symmetry. Optimized geometrical parameters are given in Table 1.

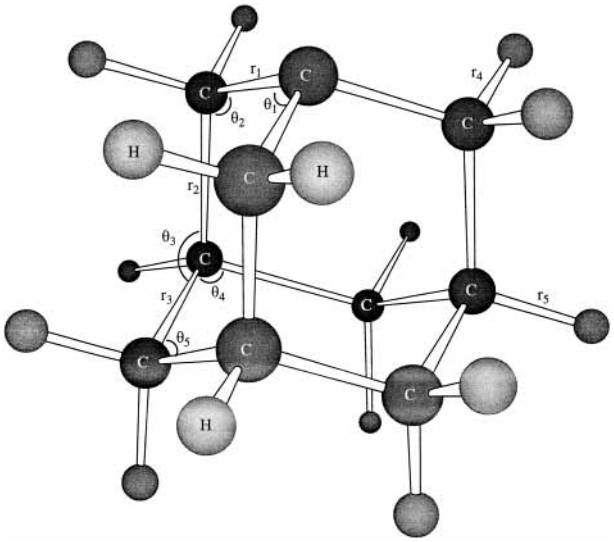

Figure 2. 1-Adamantyl radical, 1-adamantyl cation, and 1-adamantyl anion ($C_{10}H_{16}$), C_{3v} symmetry. Optimized geometrical parameters are given in Tables 2−4, respectively.

In the case of 2-Ad$^-$ (Table 7), C_s symmetry is found for the ground-state rather than the more symmetrical C_{2v} structure. The vibrational frequency analysis shows a C_{2v} imaginary frequency (553i cm^{-1} with the B3LYP method) for the out-of-plane bending mode of the C$^-$−H bond for the 2-Ad$^-$ structure, leading to the C_s minimum. The potential energy surface is found to be rather flat, with an energy difference of 20.0 kJ mol^{-1} between the C_{2v} and C_s structures at the DZP++/B3LYP level. The geometry change at the formal anionic site is similar to that of 1-Ad$^-$. The C$^-$−C$_\alpha$ bond length was shortened by 0.010 Å and the C$_\alpha$−C$^-$−C$_\alpha$ angle is decreased by 1.5°, while the C$_\alpha$−C$_\beta$ bond length is increased by 0.019 Å and the C$^-$−C$_\alpha$−C$_\beta$ angle decreased by 3.3°. The 1-Ad$^-$ anion is 2.6

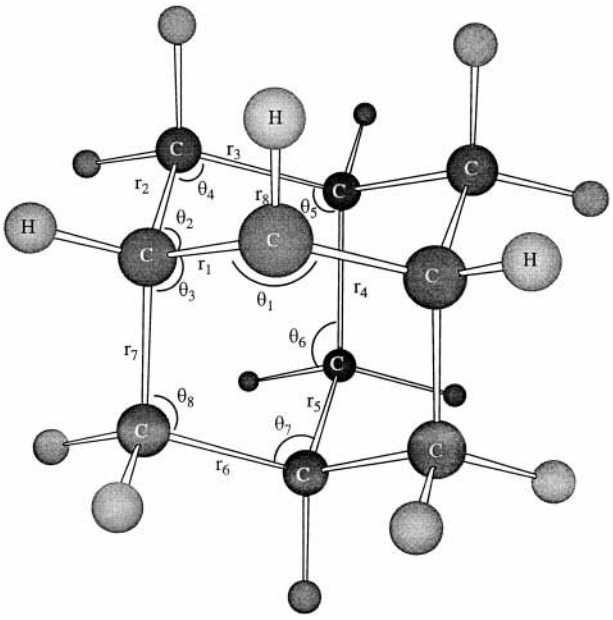

Figure 3. 2-Adamantyl radical, 2-adamantyl cation, and 2-adamantyl anion ($C_{10}H_{16}$), C_s symmetry. Optimized geometrical parameters are given in Tables 5−7, respectively.

TABLE 1: Optimized Geometry of Adamantane ($C_{10}H_{16}$, T_d)[a]

method	B3LYP	BHLYP	BLYP	BP86	experiment[b]
r_1	1.544	1.533	1.557	1.549	1.540 ± 0.002
r_2	1.100	1.091	1.108	1.109	1.112 ± 0.004
r_3	1.101	1.092	1.108	1.109	1.112 ± 0.004
θ_1	109.4	109.3	109.4	109.4	109.8 ± 0.5
θ_2	109.7	109.7	109.7	109.7	108.8 ± 1

[a] Bond lengths are in Å bond angles are in degrees. Geometric parameters correspond to those labeled in Figure 1. [b] Reference 10.

TABLE 2: Optimized Structures of the 1-Adamantyl Radical ($C_{10}H_{15}$, C_{3v})[a]

method	B3LYP	BHLYP	BLYP	BP86
r_1	1.509	1.502	1.518	1.512
r_2	1.563	1.548	1.579	1.569
r_3	1.545	1.534	1.558	1.550
r_4	1.100	1.091	1.107	1.109
r_5	1.101	1.091	1.109	1.110
θ_1	113.0	112.9	113.1	113.1
θ_2	106.0	106.1	106.0	105.9
θ_3	108.9	109.0	108.8	108.8
θ_4	109.6	109.5	109.7	109.6
θ_5	110.2	110.2	110.1	110.2

[a] Bond lengths are in Å and bond angles are in degrees. Geometric parameters correspond to those labeled in Figure 2.

TABLE 3: Optimized Structures of the 1-Adamantyl Cation ($C_{10}H_{15}$, C_{3v})[a]

method	B3LYP	BHLYP	BLYP	BP86
r_1	1.461	1.454	1.470	1.465
r_2	1.626	1.604	1.648	1.634
r_3	1.537	1.527	1.548	1.540
r_4	1.093	1.085	1.100	1.102
r_5	1.096	1.087	1.104	1.105
θ_1	117.9	117.9	117.8	117.8
θ_2	98.7	98.5	99.0	98.8
θ_3	108.2	108.4	108.0	108.0
θ_4	111.4	111.1	111.7	111.7
θ_5	109.8	109.7	109.9	109.9

[a] Bond lengths are in Å and bond angles are in degrees. Geometric parameters correspond to those labeled in Figure 2.

TABLE 4: Optimized Structures of the 1-Adamantyl Anion ($C_{10}H_{15}$, C_{3v})[a]

method	B3LYP	BHLYP	BLYP	BP86
r_1	1.525	1.524	1.530	1.525
r_2	1.558	1.547	1.569	1.561
r_3	1.545	1.533	1.558	1.550
r_4	1.109	1.099	1.117	1.118
r_5	1.112	1.100	1.122	1.123
θ_1	108.8	107.6	109.9	109.6
θ_2	111.2	112.3	110.0	110.4
θ_3	108.7	108.9	108.6	108.6
θ_4	109.3	109.2	109.5	109.5
θ_5	110.0	109.8	110.2	110.2

[a] Bond lengths are in Å and bond angles are in degrees. Geometric parameters correspond to those labeled in Figure 2.

TABLE 5: Optimized Structures of the 2-Adamantyl Radical ($C_{10}H_{15}$, C_s)[a]

method	B3LYP	BHLYP	BLYP	BP86
r_1	1.505	1.499	1.512	1.507
r_2	1.560	1.545	1.567	1.558
r_3	1.545	1.534	1.558	1.549
r_4	1.544	1.532	1.557	1.549
r_5	1.544	1.533	1.557	1.548
r_6	1.545	1.533	1.558	1.549
r_7	1.552	1.538	1.575	1.565
r_8	1.090	1.081	1.097	1.098
θ_1	114.1	113.8	114.3	114.2
θ_2	108.6	108.0	109.1	109.0
θ_3	109.1	109.0	108.3	108.2
θ_4	108.1	109.5	109.5	109.5
θ_5	109.4	109.3	109.4	109.4
θ_6	109.6	109.7	109.6	109.6
θ_7	109.9	109.4	109.4	109.3
θ_8	109.3	109.7	109.4	109.4

[a] Bond lengths are in Å and bond angles are in degrees. Geometric parameters correspond to those labeled in Figure 3.

(B3LYP), −2.1 (BHLYP), 6.6 (BLYP), and 5.5 (BP86) kJ mol^{-1} lower in energy than the 2-isomer, respectively.

For the radical 1-Ad$^\bullet$ (Table 2)**,** the ground state is found to have C_{3v} symmetry. The geometry change at the radical site with respect to the neutral Ad is quite substantial. At the DZP++/B3LYP level, the C$^\bullet$−C$_\alpha$ bond length was shortened by 0.044 Å and the C$_\alpha$−C$^\bullet$−C$_\alpha$ angle is increased by 3.6° upon the removal of one proton from the neutral Ad, whereas the C$_\alpha$−C$_\beta$ bond length is increased by 0.019 Å and C$^\bullet$−C$_\alpha$−C$_\beta$ angle decreased by 3.7°.

The ground state of 2-Ad$^\bullet$ is also found in C_s symmetry (Table 5). At the DZP++/B3LYP level, The C$^\bullet$−C$_\alpha$ bond length was shortened by 0.029 Å and the C$_\alpha$−C$^\bullet$−C$_\alpha$ angle is increased by 5.9° upon the removal of one electron from the formal anionic site of 2-Ad$^-$. The potential energy surface near the minimum is rather flat, with only a 0.23 kJ mol^{-1} energy difference between the C_s and C_{2v} isomers with the B3LYP functional. Bond lengths and bond angles for the two structures are quite similar. However, the dihedral angle between the C$_\alpha$−C$^\bullet$−C$_\alpha$ plane and the α-H of the C_s structure was decreased by 19.3° from the 180° value for the C_{2v} structure. The 1-Ad$^\bullet$ radical is 3.0 (B3LYP), 1.2 (BHLYP), 4.4 (BLYP), and 4.7 (BP86) kJ mol^{-1} lower in energy than the 2-isomer, respectively.

The ground state of the cation 1-Ad$^+$ is found to possess C_{3v} symmetry (Table 3). The geometry change at what was the radical site prior to ionization is quite substantial. At the DZP++/B3LYP level, the C$^+$−C$_\alpha$ bond length is shorter by 0.048 Å and the C$_\alpha$−C$^+$−C$_\alpha$ angle is increased by 4.9° upon the removal of the electron from the radical site of 1-Ad$^\bullet$. The

TABLE 6: Optimized Structures of the 2-Adamantyl Cation ($C_{10}H_{15}$, C_s)[a]

molecule	B3LYP	BHLYP	BLYP	BP86
r_1	1.445	1.439	1.454	1.450
r_2	1.638	1.613	1.662	1.647
r_3	1.530	1.522	1.539	1.532
r_4	1.544	1.532	1.557	1.548
r_5	1.543	1.532	1.556	1.548
r_6	1.540	1.530	1.552	1.544
r_7	1.547	1.535	1.562	1.551
r_8	1.095	1.086	1.102	1.103
θ_1	119.9	120.0	119.7	119.7
θ_2	97.7	97.4	98.6	97.7
θ_3	114.6	114.3	114.5	114.8
θ_4	108.2	108.6	107.9	108.0
θ_5	111.2	110.9	111.4	111.5
θ_6	109.8	109.9	109.5	109.5
θ_7	109.8	109.8	109.8	109.7
θ_8	109.9	109.9	109.9	109.9

[a] Bond lengths are in Å and bond angles are in degrees. Geometric parameters correspond to those labeled in Figure 3.

TABLE 7: Optimized Structures of the 2-Adamantyl Anion ($C_{10}H_{15}$, C_s)[a]

molecule	B3LYP	BHLYP	BLYP	BP86
r_1	1.534	1.530	1.540	1.535
r_2	1.563	1.549	1.576	1.567
r_3	1.547	1.535	1.561	1.553
r_4	1.545	1.534	1.557	1.549
r_5	1.545	1.534	1.558	1.550
r_6	1.546	1.534	1.559	1.551
r_7	1.549	1.537	1.563	1.554
r_8	1.110	1.093	1.108	1.110
θ_1	108.2	107.5	109.2	108.8
θ_2	112.6	113.0	111.9	112.3
θ_3	109.5	109.4	109.7	109.5
θ_4	109.2	109.4	109.0	109.1
θ_5	108.9	109.0	108.9	108.9
θ_6	109.6	109.6	109.6	109.6
θ_7	109.1	109.0	109.1	109.0
θ_8	109.4	109.5	109.4	109.4

[a] Bond lengths are in Å and bond angles are in degrees. Geometric parameters correspond to those labeled in Figure 3.

$C_\alpha-C_\beta$ bond length is increased by 0.063 Å and the $C^+-C_\alpha-C_\beta$ angle is decreased by 7.3°.

For the 2-Ad$^+$ cation, Dutler, et al. used the MP2/6-31G* method and suggested a ground electronic state with C_s symmetry rather than the more symmetric C_{2v} symmetry.[17] This is confirmed by the present research (Table 6). The energy difference between the C_{2v} and C_s structures is 7.1 kJ mol^{-1} at the DZP++/B3LYP level. The geometry change at the formal cationic site is similar to that of the 1-Ad$^+$. A natural bond orbital analysis has been performed on the 2-Ad$^+$ cation and a positive natural charge of 0.270 was found at what was the radical site prior to ionization. Compared with 2-Ad$^\bullet$, the C^+-C_α bond length is shorter by 0.060 Å and the $C_\alpha-C^+-C_\alpha$ angle has increased by 5.9° upon the removal of the electron from the radical site, and the $C_\alpha-C_\beta$ bond length is lengthened by 0.078 Å and the $C^+-C_\alpha-C_\beta$ angle decreased by 10.8°. The 1-Ad$^+$ cation is found to be 47.4 (B3LYP), 46.3 (BHLYP), 47.5 (BLYP), and 49.0 (BP86) kJ mol^{-1} lower in energy than the 2-isomer, respectively.

At the DZP++/B3LYP level, 1-Ad$^\bullet$ was found to be lowest in energy among 1-Ad$^\bullet$, Ad$^+$ and Ad$^-$ (Table 8). The energy difference between 1-Ad$^\bullet$ and 1-Ad$^-$ is quite small, with 1-Ad$^-$ predicted to lie only 12.9 kJ mol^{-1} higher than 1-Ad$^\bullet$. 1-Ad$^+$ is of course much higher in energy than the neutral radical, lying 591.6 kJ mol^{-1} above the neutral. These energy differences are similar for the case of the 2-Ad series (Table 9), with 2-Ad$^-$ lying 12.5 kJ mol^{-1} higher in energy than 2-Ad$^\bullet$, and 2-Ad$^+$ 636.0 kJ mol^{-1} above 2-Ad$^\bullet$. This energy ordering is consistent with the predicted ordering at the BHLYP and BLYP levels of theory. However, using DZP++/BHLYP level of theory, much larger energy differences between the anions and the neutral radicals are predicted. Both 1-Ad$^-$ and 2-Ad$^-$ were both found to lie about 50 kJ mol^{-1} above that of their radical counterparts. It is clear that the electron affinities of both the 1- and 2-adamantyl radicals are close to zero, explaining the difficulty observed in preparing the anions.

B. Ionization Potentials. Adiabatic and vertical ionization potentials (IP_a, IP_v) were computed and are shown in Table 10. For 1-Ad$^\bullet$, the IP_a predicted by four different functionals range from 5.84 eV (BLYP) to 6.13 eV (B3LYP). Zero-point vibrational energy (ZPVE) corrections by the B3LYP method added 0.03 eV to the results. With the ZPVE corrections, all but the BLYP functional are within 0.02 eV of the photoelectron spectroscopy result reported by Kruppa and Beauchamp,[12] which is 6.21 ± 0.03 eV. BLYP underestimates the ionization potentials by 0.34 eV, and BHLYP gives the closest agreement with the experimental result. The IP_v of 1-Ad$^\bullet$ is larger than the IP_a by as much as 0.60 (B3LYP), 0.66 (BHLYP), 0.53 (BLYP), and 0.54 (BP86) eV, respectively. This is attributed to the significant differences between the geometries of 1-Ad$^\bullet$ and 1-Ad$^+$. BHLYP overestimates the IP_a of 1-Ad$^\bullet$ by almost 0.5 eV, and BLYP (6.37 eV) gives the best agreement with experiment (6.36 ± 0.05 eV).[12]

For 2-Ad$^\bullet$, the BHLYP result of 6.70 eV (6.66 eV without ZPVE corrections) was found to give the best agreement with the experimental IP_a of 6.73 ± 0.03 eV. The B3LYP and BP86 values are both within 0.20 eV of the experimental value, while BLYP underestimates the IP_a by 0.41 eV. The BHLYP and B3LYP results are within 0.1 eV of the experimental IP_v of 2-Ad$^\bullet$ (6.99 ± 0.05 eV). BP86 underestimates the IP_v by 0.16 eV, and BLYP underestimates it by almost 0.40 eV.

C. Electron Affinities. Adiabatic and vertical electron affinities and vertical detachment energies (EA_a, EA_v, VDE) of the adamantyl radicals are shown in Table 11. For 1-Ad$^\bullet$, the predicted adiabatic EAs range from −0.55 (BHLYP) to 0.07 eV (BP86). Only the BP86 functional gives a positive EA. ZPVE corrections increase the EA_a by as much as 0.14 eV. This is an expected result of the anions being more loosely held together entities. Rienstra-Kiracofe, Barden, Brown, and Schaefer[29] used DFT to study the EAs of several polycyclic aromatic hydrocarbons including benzene, naphthalene, anthracene, tetracene, and perinaphthenyl radical, and comparable ZPVE corrections were found for their systems.

The EA_v differs considerably from the EA_a for 1-Ad$^\bullet$. This is attributed to the significant geometry difference between 1-Ad$^\bullet$ and 1-Ad$^-$. All four functionals predicted a negative EA_v, with the most negative value (−0.77 eV) reported by the BHLYP functional and the least negative value (−0.04 eV) by the BP86 functional. The geometry difference between 1-Ad$^\bullet$ and 1-Ad$^-$ also leads to VDEs that are quite different from the adiabatic EAs. Only BHLYP predicted a negative value (−0.24 eV) for the VDE of 1-Ad$^\bullet$ while the other three functionals predicted positive VDEs, with the largest value (0.23 eV) reported by the BP86 functional. The dipole moment of 1-Ad$^\bullet$ at the 1-Ad$^-$ equilibrium geometry is predicted to be 1.1 D; thus the 1-Ad$^-$ anion would not be dipole bound.

The adiabatic EAs of 2-Ad$^\bullet$ are quite similar to those of 1-Ad$^\bullet$. BHLYP gives the lowest value of −0.51 eV, followed by B3LYP (−0.13 eV) and BLYP (−0.07 eV). BP86 is the only

TABLE 8. Total Electronic Energies in hartrees and Relative Electronic Energies in kJ mol^{-1} of the 1-Adamantyl Cation, Anion, and Radical[a]

method	B3LYP		BHLYP		BLYP		BP86	
1-Ad$^+$	−389.89031	591.6	−389.65228	597.1	−389.65106	563.1	−389.87865	583.2
1-Ad$^-$	−390.11070	12.9	−389.85967	52.6	−389.86373	4.7	−390.10341	−6.9
1-Ad$^\bullet$	−390.11563	0.0	−389.87971	0.0	−389.86551	0.0	−390.10080	0.0

[a] Total energies of each system are followed by the relative energies.

TABLE 9: Total Electronic Energies in hartrees and Relative Electronic Energies in kJ mol^{-1} of the 2-Adamantyl Cation, Anion, and Radical[a]

method	B3LYP		BHLYP		BLYP		BP86	
2-Ad$^+$	−389.87227	636.0	−389.63465	642.2	−389.63298	606.1	−389.86001	627.5
2-Ad$^-$	−390.10973	12.5	−389.86047	49.3	−389.86121	6.9	−390.10131	−6.0
2-Ad$^\bullet$	−390.11449	0.0	−389.87925	0.0	−389.86384	0.0	−390.09901	0.0

[a] Total energies of each system are followed by the relative energies.

TABLE 10: Adiabatic Ionization Potentials (in eV) of the 1- and 2-Adamantyl Radicals[a]

molecule	B3LYP	BHLYP	BLYP	BP86	experiment[b]
1-Ad$^\bullet$	6.13	6.19	5.84	6.04	
	(6.16)	(6.22)	(5.87)	(6.08)	6.21± 0.03
	6.73	**6.85**	**6.37**	**6.58**	**6.36 ± 0.05**
2-Ad$^\bullet$	6.59	6.66	6.28	6.50	
	(6.63)	(6.70)	(6.32)	(6.55)	6.73± 0.03
	6.97	**7.08**	**6.60**	**6.83**	**6.99 ± 0.05**

[a] Zero-point energy corrected values are listed in parentheses. Vertical ionization potentials are listed in boldface. [b] Reference 11.

TABLE 11: Adiabatic Electron Affinities (in eV) of the 1- and 2-Adamantyl Radicals[a]

molecule	B3LYP	BHLYP	BLYP	BP86
1-Ad$^\bullet$	−0.13	−0.55	−0.05	0.07
	(0.00)	(−0.41)	(0.08)	(0.21)
	−0.28	**−0.77**	**−0.14**	**−0.04**
	0.07	*−0.24*	*0.08*	*0.23*
2-Ad$^\bullet$	−0.13	−0.51	−0.07	0.06
	(−0.04)	(−0.42)	(0.01)	(0.16)
	−0.37	**−0.82**	**−0.27**	**−0.15**
	0.22	*−0.09*	*0.20*	*0.37*

[a] Zero-point energy corrected values are listed in parentheses. Vertical electron affinities are listed in bold face, and vertical detachment energy are in italics.

functional to give a positive EA_a (0.06 eV). The B3LYP ZPVE correction is 0.09 eV. The vertical EAs are also negative for 2-Ad$^\bullet$ using each functional. BHLYP gives the lowest EA_v. −0.82 eV, while BP86 gives the highest value, −0.15 eV. For the VDEs, only BHLYP predicted a negative value of −0.09 eV, while the other three functionals predicted positive VDEs.

D. Vibrational Frequencies. The observed and computed vibrational frequencies of Ad are given in Table 12. The vibrational frequencies of 1- and 2- Ad$^\bullet$, Ad$^+$, and Ad$^-$ computed by the B3LYP method are given in Tables 13 and 14. Bistričić, Baranović, and Mlinarić-Majerski have reported Raman and infrared spectra, as well as a scaled semiempirical force field based on the vibrational assignments for Ad.[30] In our reported DFT harmonic vibrational frequencies without scaling factors, the qualitative agreement with the experiment is good. The B3LYP, BLYP, and BP86 functionals all give mean absolute errors of less than 50 cm^{-1}. The BHLYP functional is the worst in predicting the vibrational frequencies, with the largest mean absolute error (98 cm^{-1}), as one might expect because BHLYP includes 50% Hartree−Fock exchange. No experimental vibrational spectra for 1- and 2- Ad$^\bullet$, Ad$^+$, or Ad$^-$ have been reported, and we have predicted their harmonic

TABLE 12: Observed and Computed Vibrational Wavenumbers ω_e (in cm^{-1}) for Adamantane[a]

mode	sym	expt[b]	B3LYP	BHLYP	BLYP	BP86
ω_1	A_1	2950	3048	3147	2964	2972
ω_2	A_1	2913	3013	3109	2930	2937
ω_3	A_1	1472	1519	1573	1480	1467
ω_4	A_1	990	1049	1093	1015	1015
ω_5	A_1	756	755	787	726	741
ω_6	A_2	1189	1124	1165	1092	1088
ω_7	E	2900	3015	3109	2934	2941
ω_8	E	1439	1483	1536	1446	1429
ω_9	E	1370	1401	1464	1351	1356
ω_{10}	E	1217	1228	1277	1190	1189
ω_{11}	E	953	922	959	887	906
ω_{12}	E	402	412	422	403	402
ω_{13}	T_1		3054	3149	2971	2984
ω_{14}	T_1	1321	1341	1399	1299	1291
ω_{15}	T_1	1288	1317	1380	1266	1276
ω_{16}	T_1	-	1125	1170	1091	1086
ω_{17}	T_1	1043	1060	1103	1018	1035
ω_{18}	T_1	-	901	932	876	871
ω_{19}	T_1	-	340	341	335	338
ω_{20}	T_2	2940	3060 (109)	3156 (109)	2976 (117)	2987 (102)
ω_{21}	T_2	2910	3037 (179)	3135 (163)	2952 (207)	2962 (186)
ω_{22}	T_2	2850	3015 (38)	3109 (43)	2933 (26)	2939 (47)
ω_{23}	T_2	1455	1497 (11)	1550 (11)	1459 (10)	1444 (12)
ω_{24}	T_2	1359	1380	1440	1336	1331
ω_{25}	T_2	1310	1340	1408	1284	1292
ω_{26}	T_2	1101	1115 (3)	1159 (3)	1081 (3)	1081 (3)
ω_{27}	T_2	970	981 (1)	1018 (1)	948 (1)	957 (2)
ω_{28}	T_2	800	817 (1)	846 (1)	788	805 (1)
ω_{29}	T_2	638	657	678	639	639
ω_{30}	T_2	444	458	467	449	447

[a] Infrared intensities (in km mol^{-1}) larger than 1 km mol^{-1} are shown in parentheses following the wavenumbers. [b] Reference 30.

vibrational frequencies using the B3LYP method. The vibrational frequencies of the adamantyl anions are generally smaller than those of the radicals, while the adamantyl cations have the largest vibrational frequencies for the same modes, compared with the anions and neutral radicals.

IV. Conclusions

In the extensive review of Rienstra-Kiracofe, Tschumper, and Schaefer[19] on the electron affinities from photoelectron experiments and theoretical computations, it was found that DFT EA results tend to overestimate experimental values for all but the BHLYP functional. Rienstra-Kiracofe et al.[19] also found that for the EAs in closed-shell anion to open-shell neutral systems (like 1- and 2- Ad$^-$ to Ad$^\bullet$), the B3LYP functional gives the smallest average absolute errors compared to experimental

TABLE 13: Harmonic Vibrational Wavenumbers ω_e (in cm^{-1}) for the 1-Adamantyl Radical, Anion, and Cation by the B3LYP Method[a]

mode	sym	1-Ad$^{\bullet}$	1-Ad^{-}	1-Ad^{+}
ω_1	A_1	3060 (105)	2984 (28)	3109 (6)
ω_2	A_1	3044 (15)	2969 (86)	3106 (1)
ω_3	A_1	3023 (99)	2910 (9)	3099 (1)
ω_4	A_1	3012 (7)	2869 (238)	3063 (1)
ω_5	A_1	1509	1492 (1)	1540 (3)
ω_6	A_1	1491 (12)	1448	1496 (15)
ω_7	A_1	1349	1334 (9)	1320 (4)
ω_8	A_1	1266 (5)	1242 (14)	1203 (61)
ω_9	A_1	1097 (5)	1085	1081 (29)
ω_{10}	A_1	1028 (1)	997 (28)	1010 (10)
ω_{11}	A_1	924 (1)	918 (37)	882 (3)
ω_{12}	A_1	778 (3)	761 (45)	826 (1)
ω_{13}	A_1	757 (1)	742 (27)	766 (3)
ω_{14}	A_1	636 (6)	556 (220)	682 (16)
ω_{15}	A_1	439	404 (62)	468
ω_{16}	A_2	3065	2942	3169
ω_{17}	A_2	1337	1332	1335
ω_{18}	A_2	1303	1302	1290
ω_{19}	A_2	1124	1114	1130
ω_{20}	A_2	1110	1108	1087
ω_{21}	A_2	1048	1048	1050
ω_{22}	A_2	901	874	927
ω_{23}	A_2	311	328	289
ω_{24}	E	3071 (89)	2989 (133)	3175 (2)
ω_{25}	E	3054 (12)	2958 (272)	3104 (11)
ω_{26}	E	3034 (196)	2945 (149)	3102 (4)
ω_{27}	E	3018 (6)	2905 (778)	3096 (1)
ω_{28}	E	3013 (14)	2880 (324)	3059 (8)
ω_{29}	E	1487 (11)	1476 (2)	1520 (23)
ω_{30}	E	1476	1447 (2)	1475 (12)
ω_{31}	E	1387	1377 (12)	1411 (2)
ω_{32}	E	1362	1353 (2)	1381 (1)
ω_{33}	E	1333	1313 (21)	1351 (6)
ω_{34}	E	1294 (1)	1274 (19)	1276 (5)
ω_{35}	E	1260	1242 (1)	1210 (18)
ω_{36}	E	1173	1161 (3)	1135
ω_{37}	E	1113 (3)	1100 (36)	1095 (13)
ω_{38}	E	1041	1034 (22)	1020 (16)
ω_{39}	E	984 (2)	976 (28)	983 (9)
ω_{40}	E	920	909 (8)	895
ω_{41}	E	890	888 (5)	859 (17)
ω_{42}	E	799	787 (26)	737 (5)
ω_{43}	E	638 (1)	651	569 (19)
ω_{44}	E	447	447	460 (1)
ω_{45}	E	395	406	358 (8)
ω_{46}	E	320	315 (2)	337 (4)

[a] Infrared intensities (in km mol^{-1}) larger than 1 km mol^{-1} are shown in parentheses following the wavenumbers.

results. Therefore, it is reasonable to argue that the true electron affinities for the systems studied here should lie between the predicted values of BHLYP and the other functionals and should be closest to the B3LYP predicted values. Also we have found that the ZPVE corrections are as large as 0.13 eV for the 1-Ad$^{\bullet}$ and 0.10 eV for the 2-Ad$^{\bullet}$. However, the negative EAs suggested nonbound anions, and ZPVE corrections are not necessary for these cases. Therefore, it is reasonable to give theoretical predictions for EAs from the B3LYP results without ZPVE corrections. Our final predicted values are as follows: EA_a -0.13 eV(1- and 2-Ad$^{\bullet}$); EA_v -0.28 eV(1-Ad$^{\bullet}$), -0.37 eV(2-Ad$^{\bullet}$); VDE 0.07 eV(1-Ad$^{\bullet}$), 0.22 eV(2-Ad$^{\bullet}$). It is clear that the adamantyl radicals do not readily attract an electron. Of course, suitable substituted adamantyl radicals are expected to have positive electron affinities.

Acknowledgment. This work was supported by the Department of Energy, through its Combustion and SciDAC Research Programs. We thank the DOE NERSC computing center for continuing support.

TABLE 14: Harmonic Vibrational Wavenumbers ω_e (in cm^{-1}) for the 2-Adamantyl Radical, Anion, and Cation by the B3LYP Method[a]

mode	sym	2-Ad$^{\bullet}$	2-Ad^{-}	2-Ad^{+}
ω_1	A′	3178 (35)	3054 (47)	3160
ω_2	A′	3068 (79)	3031 (97)	3129 (12)
ω_3	A′	3063 (94)	2991 (167)	3116 (4)
ω_4	A′	3057 (2)	2977 (89)	3113 (14)
ω_5	A′	3042 (127)	2966 (28)	3087 (14)
ω_6	A′	3036 (128)	2959 (109)	3074 (7)
ω_7	A′	3017 (4)	2941 (26)	3066 (8)
ω_8	A′	3014 (19)	2916 (281)	3058 (17)
ω_9	A′	3012 (20)	2865 (771)	3045 (4)
ω_{10}	A′	1508 (2)	1494 (2)	1518 (2)
ω_{11}	A′	1485 (10)	1467 (25)	1497 (16)
ω_{12}	A′	1482 (4)	1466 (15)	1487 (7)
ω_{13}	A′	1394	1374 (1)	1440 (11)
ω_{14}	A′	1377	1361 (1)	1380
ω_{15}	A′	1375	1349 (9)	1369 (1)
ω_{16}	A′	1337	1326 (1)	1345 (4)
ω_{17}	A′	1326	1311 (19)	1322
ω_{18}	A′	1318	1296 (3)	1318
ω_{19}	A′	1271	1261 (6)	1228 (17)
ω_{20}	A′	1225	1201 (8)	1180 (9)
ω_{21}	A′	1124	1110	1128 (2)
ω_{22}	A′	1103 (2)	1090 (4)	1108 (5)
ω_{23}	A′	1063 (1)	1066 (2)	1077 (7)
ω_{24}	A′	1046	1041 (1)	1056 (2)
ω_{25}	A′	1023 (1)	1016 (1)	1018 (4)
ω_{26}	A′	964 (2)	959 (3)	982 (11)
ω_{27}	A′	947 (2)	933 (1)	948 (4)
ω_{28}	A′	911	900	929 (2)
ω_{29}	A′	816 (1)	804 (5)	875 (19)
ω_{30}	A′	799 (1)	787 (10)	810 (1)
ω_{31}	A′	759	749 (2)	791 (1)
ω_{32}	A′	681 (2)	731 (129)	742 (3)
ω_{33}	A′	652	647 (5)	667 (16)
ω_{34}	A′	535 (10)	628 (105)	619 (1)
ω_{35}	A′	438	461 (8)	443
ω_{36}	A′	406	441 (6)	435 (6)
ω_{37}	A′	349 (4)	393 (36)	372 (4)
ω_{38}	A′	214 (17)	317 (12)	326 (7)
ω_{39}	A″	3066 (26)	3049	3127
ω_{40}	A″	3060 (5)	3026 (6)	3117 (1)
ω_{41}	A″	3056 (152)	3009 (99)	3111 (11)
ω_{42}	A″	3055 (24)	2966 (461)	3102 (12)
ω_{43}	A″	3018 (78)	2946 (18)	3070 (3)
ω_{44}	A″	3013 (31)	2869 (617)	3064 (15)
ω_{45}	A″	1486 (11)	1465	1515 (32)
ω_{46}	A″	1470	1452 (6)	1480
ω_{47}	A″	1381	1381	1465 (2)
ω_{48}	A″	1374	1349 (1)	1387
ω_{49}	A″	1341	1321	1346
ω_{50}	A″	1333	1316	1325 (12)
ω_{51}	A″	1321	1306 (1)	1307
ω_{52}	A″	1304	1258 (13)	1292 (6)
ω_{53}	A″	1261	1244 (8)	1201 (12)
ω_{54}	A″	1161	1153	1178 (1)
ω_{55}	A″	1125 (1)	1112 (1)	1160
ω_{56}	A″	1122	1102 (7)	1111
ω_{57}	A″	1112 (3)	1094 (4)	1098 (2)
ω_{58}	A″	1069	1049 (11)	1063 (15)
ω_{59}	A″	1050	1026 (17)	990 (35)
ω_{60}	A″	983 (1)	977 (3)	976 (5)
ω_{61}	A″	906	899	896
ω_{63}	A″	896	895 (2)	877
ω_{63}	A″	884	862 (1)	844 (22)
ω_{64}	A″	797	786	666 (18)
ω_{65}	A″	644	646 (1)	581 (26)
ω_{66}	A″	446	447	441 (1)
ω_{67}	A″	401	406	353 (5)
ω_{68}	A″	313	322	301
ω_{69}	A″	305	317 (1)	169 (27)

[a] Infrared intensities (in km mol^{-1}) larger than 1 km mol^{-1} are shown in parentheses following the wavenumbers.

References and Notes

(1) Schleyer, P. v. R. *J. Am. Chem. Soc.* **1957**, *79*, 3292.

(2) Beller, M.; Ehrentraut, A.; Fuhrmann, C.; Zapf, A. *PCT Int. Appl.* **2002**, 41.

(3) Taoufik, M.; Santini, C. C.; Basset, J.-M. *J. Organomet. Chem.* **1999**, *580*, 128.

(4) Jeong, H. Y.; Lee, Y. K.; Talaie, A.; Kim, K. M.; Kwon, Y. D.; Jang, Y. R.; Yoo, K. H.; Choo, D. J.; Jang, J. *Thin Solid Films* **2002**, *417*, 171.

(5) Mathias, L. J.; Jensen, J. J.; Reichert, V. R.; Lewis, C. M.; Tullos, G. L. *Polym. Prepr. (Am. Chem. Soc., Div. Polym. Chem.)* **1995**, *36*, 741.

(6) Stotskaya, L. L.; Serbin, A. V.; Munshi, K.; Kozeletskaya, K. N.; Sominina, A. A.; Kiselev, O. I.; Zaitseva, K. V.; Natochin, Y. V. *Khim.-Farm. Zh.* **1995**, *29*, 19.

(7) Boukrinskaia, A. G.; Serbin, A. V.; Bogdan, O. P.; Stotskaya, L. L.; Alymova, I. V.; Klimochkin, Y. N. *PCT Int. Appl.* **1995**, 32.

(8) Ruppersberg, J. P.; Fakler, B. P. *PCT Int. Appl.* **2002**, 31.

(9) Spasov, A. A.; Khamidova, T. V.; Bugaeva, L. I.; Morozov, I. S. *Pharm. Chem. J. (*translation of *Khim.-Farm. Zh.)* **2000**, *34*, 1.

(10) Hargittai, I.; Hedberg, K. In *Molecular Structures and Vibrations*; Cyvin, S. J., Ed.; Elsevier: **1972**, p 340.

(11) Tian, S. X.; Kishimoto, N.; K.; H. *J. Phys. Chem. A* **2002**, *106*, 6541.

(12) Kruppa, G. H.; Beauchamp, J. L. *J. Am. Chem. Soc.* **1985**, *108*, 2162.

(13) Kira, M.; Akiyama, M.; Ichinose, M.; Sakurai, H. *J. Am. Chem. Soc.* **1989**, *111*, 8256.

(14) Aubry, C.; Holmes, J. L.; Walton, J. C. *J. Phys. Chem. A* **1998**, *102*, 1389.

(15) Abboud, J.-L. M.; Castano, O.; Davalos, J. Z.; Gomperts, R. *Chem. Phys. Lett.* **2001**, *337*, 327.

(16) Bistricic, L.; Pejov, L.; Baranovic, G. *J. Mol. Struct. (THEOCHEM)* **2002**, *594*, 79.

(17) Dutler, R.; Rauk, A.; Sorensen, T. S.; Whitworth, S. M. *J. Am. Chem. Soc.* **1989**, *111*, 9024.

(18) Proft, F. D.; Geerlings, P. *J. Chem. Phys.* **1997**, *106*, 3270.

(19) Rienstra-Kiracofe, J. C.; Tschumper, G. S.; Schaefer, H. F.; Nandi, S.; Ellison, G. B. *Chem. Rev.* **2002**, *102*, 231.

(20) Gaussian 94. Revision C.3.; Frisch, M. J.; Trucks, G. W.; Schlegel, H. B.; Gill, P. M. W.; Johnson, B. G.; Robb, M. A.; Cheeseman, J. R.; Keith, T.; Petersson, G. A.; Montgomery, J. A.; Raghavachari, K.; Al-Laham, M. A.; Zakrzewski, V. G.; Ortiz, J. V.; Foresman, J. B.; Cioslowski, J.; Stefanov, B. B.; Nanayakkara, A.; Challacombe, M.; Peng, C. Y.; Ayala, P. Y.; Chen, W.; Wong, M. W.; Andres, J. L.; Replogle, E. S.; Gomperts, R.; Martin, R. L.; Fox, D. J.; Binkley, J. S.; Defrees, D. J.; Baker, J.; Stewart, J. P.; Head-Gordon, M.; Gonzalez, C.; Pople, J. A.; Gaussian, Inc.: Pittsburgh, PA, 1995.

(21) Becke, A. D. *J. Chem. Phys.* **1993**, *98*, 5648.

(22) Lee, C.; Yang, W.; Parr, R. G. *Phys. Rev. B.* **1988**, *37*, 785.

(23) Becke, A. D. *J. Chem. Phys.* **1993**, *98*, 1372.

(24) Becke, A. D. *Phys. Rev. A.* **1988**, *38*, 3098.

(25) Perdew, J. P. *Phys. Rev. B.* **1986**, *33*, 8822.

(26) Huzinaga, S. *J. Chem. Phys.* **1965**, *42*, 1293.

(27) Dunning, T. H. *J. Chem. Phys.* **1970**, *53*, 2823.

(28) Lee, T. J.; Schaefer, H. F. *J. Chem. Phys.* **1985**, *83*, 1784.

(29) Rienstra-Kiracofe, J. C.; Barden, C. J.; Brown, S. T.; Schaefer, H. F. *J. Phys. Chem. A* **2001**, *105*, 524.

(30) Bistričić, L.; Baranović, G.; Mlinarić-Majerski, K. *Spectrochim. Acta A* **1995**, *51*, 1643.